2016 IEEE International Conference on Robotics and Automation (ICRA)
Stockholm, Sweden, May 16-21, 2016

Bipedal Gait Recharacterization and Walking Encoding Generalization for Stable Dynamic Walking

Yan Gu, Bin Yao, and C. S. George Lee

Abstract— **In this paper, we propose to achieve exponentially stable periodic bipedal walking based on recharacterization of bipedal gait and generalization of walking encoding. To conveniently define an asymmetric walking pattern, a gait is characterized here in terms of the left and the right legs instead of the support and the swing legs. Another benefit of this characterization is that the joint positions become well-defined and continuous throughout a walking process even under impulse effects caused by impacts. A more general walking encoding method is then introduced, which not only includes walking pattern encoding but also enables upper-level task planning and control. Walking dynamics is then rewritten with the roles of the left and the right legs differentiated and with the biped's global position included. The desired walking pattern, as well as the desired global motion, is tracked exponentially fast through a controller designed using the output feedback linearization method. Stability of the hybrid dynamical control system is analyzed based on the construction of multiple Lyapunov functions. Finally, a fully actuated compass-gait biped is simulated to show that the proposed framework can realize exponentially stable walking, both symmetric and asymmetric, while satisfactorily tracking the desired walking pattern and the planned global motion.**

I. Introduction

Maintaining stability is the first priority of bipedal locomotion, which is defined as the ability not to fall over [1]. By this definition, viability [2] is the exact equivalence of stability for bipedal locomotion and the viability kernel contains all the states starting from which a robot never falls [1]. Capturability is a computationally less expensive approximation of viability [3]. A capture point is defined as a point where the robot can come to a complete stop by stepping on given the current state [4]. Impressive dynamic walking has been realized based on the concepts of capturability and capture points [5].

However, maintaining stability is the minimum requirement for bipedal locomotion, besides which there can be additional performance objectives such as following a certain walking pattern and minimizing energy consumption. If a biped can track the desired walking pattern satisfactorily and the control system is stable, then walking stability is achieved automatically. Asymptotically orbital stabilization of underactuated periodic bipedal walking was achieved under finite-time convergence to the desired walking pattern [6]. Later on, finite-time stabilization was relaxed to be sufficiently fast exponential stabilization [7] [8]. The aforementioned planning and control strategies and their extensions have been successfully implemented on physical bipedal systems [9] [10] [11]. Instead of using output feedback linearization and checking orbital stability through Poincaré Map, a transverse coordinate system is constructed along the desired orbit and orbital stabilization is achieved by stabilizing the linearized transverse system based on receding horizon control [12]. Another interesting study is the sums-of-squares approach which maximizes the region of attraction by utilizing quadratic programming [13]. Recently, an intuitive control strategy of dynamic bipedal walking has been successfully implemented based on energy regulation [14].

In this study, exponentially stable bipedal walking is realized based on gait recharacterization and walking encoding generalization. Bipedal-walking dynamics has been typically expressed in terms of the support and the swing legs. Here, the left and the right legs are differentiated so that an asymmetric gait can be conveniently defined. Joint positions also become continuous and well-defined upon swing foot landing. Moreover, a biped's global position with respect to the world coordinate frame is included in the dynamic model so that the previous walking pattern encoding, known as the Virtual Constraints [6], can be integrated with the biped's travel distance for upper-level planning and tracking of desired global motion. Another potential benefit is that various types of ground-contact constraints can be explicitly dealt with in the controller design but this advantage will not be explored in this study. Output feedback linearization is utilized to synthesize controllers that enforce the desired walking pattern and the desired global motion.

In Section II, problem formulation is presented, including the proposed walking characterization, the bipedal-walking dynamics, and the generalized walking pattern encoding. Controller design based on output feedback linearization is briefly introduced in Section III. The main theorem of stability with a sketch of the proof is given in Section IV based on the construction of multiple Lyapunov functions. Simulation results are presented in Section V.

II. Problem Formulation

A fully actuated planar biped walking on horizontal even terrain is considered (see Fig. 1). Its two legs are identical, and the feet are thin and massless. It is assumed that the swing foot always lands flat with a rigid impact of an

Yan Gu and Bin Yao are with the School of Mechanical Engineering, and C. S. George Lee is with the School of Electrical and Computer Engineering, Purdue University, West Lafayette, IN 47907, U.S.A. {gu49, byao, csglee}@purdue.edu. Bin Yao is also a Chang Jiang Chair Professor at the State Key Laboratory of Fluid Power and Mechatronic Systems of Zhejiang University in China.

This work was supported in part by the National Science Foundation under Grant IIS-0916807. Any opinion, findings, and conclusions or recommendations expressed in this material are those of the authors and do not necessarily reflect the views of the National Science Foundation.

infinitesimal period of time and that the double-support phases are instantaneous [6]. There are two actuators at the hip and one at each ankle. Three of them are active at any moment except for the actuator at the swing foot.

A. Gait Characterization

A symmetric bipedal gait is typically characterized by the support leg and the swing leg in previous studies [6] [8] [12]. Due to the coordinate swap, both the positions and the velocities of the support and the swing legs experience discontinuities upon a swing-foot landing even for soft touchdown. In contrast, when a gait is characterized by the left and the right legs, which is adopted in this paper, there is no coordinate swap upon a swing-foot landing. Definition of each state will be consistent, and joint positions upon an impact will be continuous and well-defined. Based on this characterization, system dynamics consists of two single-support phases, the left-leg-in-support phase and the right-leg-in-support phase, and two reset maps, the left-to-right-leg-support reset map and the right-to-left-leg-support reset map, and will be rewritten in the following subsection.

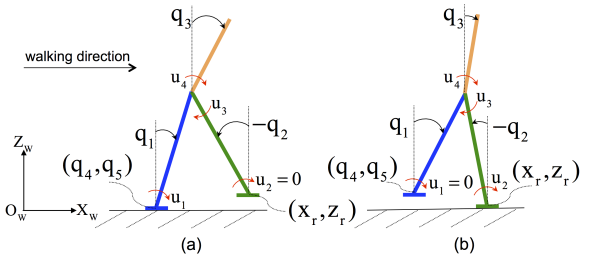

Fig. 1. A Bipedal Robot Walking in the X_w-Z_W Plane. (a): left foot in support. (b): right foot in support. Blue segment: left leg and foot. Orange segment: trunk. Green segment: right leg and foot.

B. Bipedal-walking Dynamics

1) Continuous Dynamics during Single-support Phases: Besides the three joint positions, two generalized coordinates are added to represent the biped's position in the world coordinate frame.

Denote

$$\mathbf{q} = \begin{bmatrix} q_1, & q_2, & q_3, & q_4, & q_5 \end{bmatrix}^T, \tag{1}$$

where q_1 represents the left-leg angle, q_2 the right-leg angle, q_3 the trunk angle, q_4 the left-ankle position in the X_w-direction (i.e., the forward direction) of the world coordinate frame, and q_5 the left-ankle position in the Z_w-direction (i.e., the upward direction) of the world coordinate frame (see Fig. 1). Suppose that the walking direction aligns with the positive direction of the X_w-axis and that the walking process begins with the left foot in support.

Denote

$$\mathbf{u} = \begin{bmatrix} u_1, & u_2, & u_3, & u_4 \end{bmatrix}^T, \tag{2}$$

where u_1, u_2, u_3 and u_4 are illustrated in Fig. 1.

Dynamic equations during the $(k+1)^{th}$ stride (a stride consists of two successive steps), $k \in \{0,1,2,...\}$, can be written as:

$$\mathbf{M}(\mathbf{q})\ddot{\mathbf{q}} + \mathbf{h}(\mathbf{q},\dot{\mathbf{q}}) = \mathbf{B}_{ui}\mathbf{u} + \mathbf{J}_i^T(\mathbf{q})\mathbf{F}_i, \tag{3}$$

with

$$\begin{cases} \text{left-leg-in-support:} & q_4 = \sum_0^{2k} s_j, q_5 = 0, \\ \text{right-leg-in-support:} & x_r = \sum_0^{2k+1} s_j, z_r = 0, \end{cases} \tag{4}$$

where $\mathbf{M}(\mathbf{q})$ represents the inertia matrix, $\mathbf{h}(\mathbf{q},\dot{\mathbf{q}})$ the sum of the gravitational term, the Coriolis force and the centrifugal force, $\mathbf{u}$ the joint-torque vector, the subscript $i \in \{L,R\}$ the support leg with $i = L/R$ for left/right-leg support, $\mathbf{B}_{ui}$ the joint-torque projection matrix, $\mathbf{F}_i = [F_{ix}, F_{iz}]^T$ the ground-contact force applied on the support foot, s_j ($j \in \{1,2,...\}$) the length of the last step before the j^{th} impact with s_0 defined as the initial value of q_4, i.e., $s_0 = q_4(0)$, $[x_r, z_r]^T$ the right-ankle position with respect to the world coordinate frame, and $\mathbf{J}_i(\mathbf{q})$ the Jacobian matrix which is determined by the holonomic constraints in (4).

2) Impact Dynamics during Instantaneous Double-support Phases: When the state $(\mathbf{q},\dot{\mathbf{q}})$ hits the switching surface, denoted as $S_i(\mathbf{q})$ ($i \in \{L,R\}$), the support foot and the swing foot switch their roles and the ground-contact constraint changes. Define $S_i(\mathbf{q})$ ($i \in \{L,R\}$) as [6]:

$$\begin{cases} \text{left-to-right-leg-support:} & S_L = \{\mathbf{q} : h_L(\mathbf{q}) = 0, d_L(\mathbf{q}) > 0\}, \\ \text{right-to-left-leg-support:} & S_R = \{\mathbf{q} : h_R(\mathbf{q}) = 0, d_R(\mathbf{q}) > 0\}, \end{cases}$$

where $h_i(\mathbf{q})$ is the swing-foot height and $d_i(\mathbf{q})$ the relative position of the swing foot with respect to the support foot.

When the swing leg passes the support leg, a compass-gait biped with identical fixed-length legs can only avoid scuffing the ground exactly at $q_1 = q_2 = 0$. It is thus supposed that the swing-leg length can be adjusted to avoid scuffing the ground [6]. Then, $h_L(\mathbf{q}) = l\cos(q_1) - l\cos(q_2)$ and $h_R(\mathbf{q}) = l\cos(q_2) - l\cos(q_1)$. The switching surfaces become:

$$\begin{cases} \text{left-to-right-leg-support:} & S_L = \{\mathbf{q} : q_1 + q_2 = 0, q_1 > 0\}, \\ \text{right-to-left-leg-support:} & S_R = \{\mathbf{q} : q_1 + q_2 = 0, q_2 > 0\}. \end{cases}$$

The double-support-phase dynamics is a reset map:

$$\begin{cases} \text{left-to-right-leg-support:} & \dot{\mathbf{q}}^+ = \Delta_{\dot{q}L}(\mathbf{q},\dot{\mathbf{q}}^-), \\ \text{right-to-left-leg-support:} & \dot{\mathbf{q}}^+ = \Delta_{\dot{q}R}(\mathbf{q},\dot{\mathbf{q}}^-). \end{cases} \tag{5}$$

Note that the impact map (5) does not include coordinate reset, which will be present if the support and the swing legs are used to characterize a gait. With the proposed characterization, joint positions are continuous and only joint velocities experience a sudden jump upon a rigid impact with an infinitesimally small length of time.

C. Generalized Walking Pattern Encoding

A walking pattern [6] defines the evolution of a biped's relative configuration in a complete stride which can be completely described by q_1, q_2 and q_3. A travel path is a geometrical contour defined on the ground surface and cannot be completely described by q_1, q_2 and q_3 alone. When a biped navigates in a complex environment, it is necessary to follow a certain travel path, for example, to avoid obstacles, and track the desired motion on the travel path. In previous related work [10] [15], the desired walking speed is tracked, and thus convergence to the desired global trajectory is not guaranteed.

Similar to contouring control [16], an orthogonal global task coordinate frame can be constructed along the desired travel path. In this way, the contour error and the motion along the desired contour can be separately represented in two sets of coordinates. Minimizing the contour error then

becomes a stabilization problem, and following the desired motion along the desired contour becomes a trajectory tracking problem. For planar bipedal walking, a biped is confined to walking along the X_w-axis, which is the only feasible travel path. Hence, the walking control objectives are reduced to trajectory tracking along the X_w-axis and walking pattern following. In our future work on three-dimensional walking, the complete problem of contouring control will be studied as an extension of the current study.

To define the desired motion along the travel path for planar bipedal walking, the travel distance s of the hip joint during the $(k+1)^{th}$ stride ($k \in \{0,1,2,...\}$) is introduced:

$$s = \begin{cases} q_4 + l\sin(q_1) = \sum_0^{2k} s_j + l\sin(q_1) & \text{(left-leg-in-support)}, \\ x_r + l\sin(q_2) = \sum_0^{2k+1} s_j + l\sin(q_2) & \text{(right-leg-in-support)} \end{cases} \tag{6}$$

The desired motion along the travel path is denoted as $s_d(t)$, and we want $s(t)$ to track $s_d(t)$ sufficiently well.

To integrate walking pattern encoding with a biped's global motion, the relative position $\bar{s}$ of the hip with respect to the support leg, which increases monotonically during a forward step, is used as the encoding variable:

$$\bar{s} = \begin{cases} s - q_4 & \text{(left-leg-in-support)}, \\ s - x_r & \text{(right-leg-in-support)}. \end{cases} \tag{7}$$

Note that $\bar{s} = lsin(q_{st})$ where q_{st} is the support-leg angle.

The desired walking pattern is encoded as $\mathbf{g}_i(\bar{s}, \bar{\mathbf{q}}) = \mathbf{0}$ ($i \in \{L,R\}$):

$$\begin{cases} \text{left-leg-in-support:} & \mathbf{g}_L(\bar{s}, \bar{\mathbf{q}}) := \begin{bmatrix} q_2 - \phi_{1L}(\bar{s}) \\ q_3 - \phi_{2L}(\bar{s}) \end{bmatrix} = \mathbf{0}, \\ \text{right-leg-in-support:} & \mathbf{g}_R(\bar{s}, \bar{\mathbf{q}}) := \begin{bmatrix} q_1 - \phi_{1R}(\bar{s}) \\ q_3 - \phi_{2R}(\bar{s}) \end{bmatrix} = \mathbf{0}, \end{cases} \tag{8}$$

where $\bar{\mathbf{q}} := [q_1, q_2, q_3]^T$, and $\phi_{1L}(\bar{s})$, $\phi_{2L}(\bar{s})$, $\phi_{1R}(\bar{s})$ and $\phi_{2R}(\bar{s})$ should be chosen such that $\begin{bmatrix} q_1 \\ \mathbf{g}_L(\bar{s}, \bar{\mathbf{q}}) \end{bmatrix}$ and $\begin{bmatrix} q_2 \\ \mathbf{g}_R(\bar{s}, \bar{\mathbf{q}}) \end{bmatrix}$ are both local diffeomorphisms.

Figure 2 shows two examples of walking pattern encoding. It is straightforward to see that both symmetric and asymmetric gaits can be conveniently defined by differentiating the left leg and the right leg.

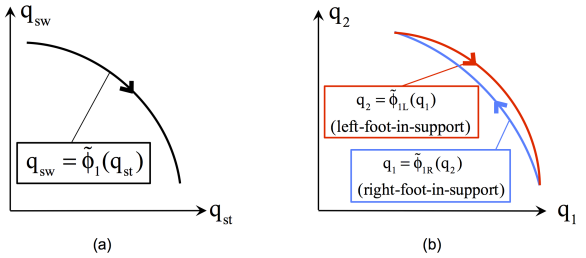

Fig. 2. Encoding the Swing-leg (q_{sw}) Pattern with Two Different Walking Characterizations. (a): using the support-leg angle q_{st} and the swing-leg angle q_{sw}. (b): using the left-leg angle q_1 and the right-leg angle q_2.

III. Output Feedback Linearization

Assume that the dynamic model is perfectly known and that there are no disturbances or noise. Output feedback linearization is thus utilized to synthesize the needed controller.

Assume that $q_4(t)$ and $x_r(t)$ are known or measured after each stride. Then, the desired trajectory for the support-leg angle corresponding to $s_d(t)$ is:

$$\begin{cases} \text{left-leg-in-support:} & q_{1d}(t) = sin^{-1}(\frac{s_d(t) - q_4}{l}), \\ \text{right-leg-in-support:} & q_{2d}(t) = sin^{-1}(\frac{s_d(t) - x_r}{l}). \end{cases} \tag{9}$$

We are now ready to define the output functions as:

$$\begin{cases} \text{left-leg-in-support:} & \mathbf{y}_L = \begin{bmatrix} q_1 - q_{1d}(t) \\ q_2 - \tilde{\phi}_{1L}(q_1) \\ q_3 - \tilde{\phi}_{2L}(q_1) \end{bmatrix}, \\ \text{right-leg-in-support:} & \mathbf{y}_R = \begin{bmatrix} q_1 - \tilde{\phi}_{1R}(q_2) \\ q_2 - q_{2d}(t) \\ q_3 - \tilde{\phi}_{2R}(q_2) \end{bmatrix}, \end{cases} \tag{10}$$

where $\tilde{\phi}_{ji}(q_{st}) = \phi_{ji}(\bar{s})$ with $i \in \{L,R\}$ and $j \in \{1,2\}$.

Then we have

$$\ddot{\mathbf{y}}_i = \mathbf{P}_i(q_i)\ddot{\bar{\mathbf{q}}} - \mathbf{z}_i(t, q_i, \dot{q}_i) \ , \ i \in \{L,R\}, \tag{11}$$

where $\mathbf{P}_i(q_i)$ is a 3×3 invertible matrix and $\mathbf{z}_i(t, q_i, \dot{q}_i)$ is a 3×1 vector.

From the continuous dynamics in (3) and the holonomic constraints in (4), we have

$$\ddot{\bar{\mathbf{q}}} = \mathbf{M}_i(\bar{\mathbf{q}})^{-1}(\mathbf{B}_i\mathbf{u}_i - \mathbf{h}_i(\bar{\mathbf{q}}, \dot{\bar{\mathbf{q}}})) \ , \ i \in \{L,R\}, \tag{12}$$

where $\mathbf{M}_i$, $\mathbf{h}_i$ and $\mathbf{B}_i$ are the dynamic matrices associated with the reduced dynamic equations and $\mathbf{u}_i$ is the vector of active joint torques.

Hence,

$$\ddot{\mathbf{y}}_i = \mathbf{N}_i(\bar{\mathbf{q}})\mathbf{u}_i - \mathbf{L}_i(t, \bar{\mathbf{q}}, \dot{\bar{\mathbf{q}}}) \ , \ i \in \{L,R\}, \tag{13}$$

where $\mathbf{N}_i = \mathbf{P}_i\mathbf{M}_i^{-1}\mathbf{B}_i$ and $\mathbf{L}_i = \mathbf{P}_i\mathbf{M}_i^{-1}\mathbf{h}_i + \mathbf{z}_i$.

Since $\mathbf{N}_i$ is invertible, the linearization control law

$$\mathbf{u}_i = \mathbf{N}_i^{-1}(\mathbf{v}_i + \mathbf{L}_i) \tag{14}$$

results in

$$\ddot{\mathbf{y}}_i = \mathbf{v}_i \ , \ i \in \{L,R\}, \tag{15}$$

where $\mathbf{v}_i$ can be chosen as a PD controller:

$$\mathbf{v}_i = -\mathbf{K}_{Pi}\mathbf{y}_i - \mathbf{K}_{Di}\dot{\mathbf{y}}_i, \ , \ i \in \{L,R\}, \tag{16}$$

where $\mathbf{K}_{Pi}$ and $\mathbf{K}_{Di}$ are diagonal matrices of proportional gains and derivative gains, respectively. The linearized dynamics then becomes:

$$\dot{\mathbf{x}} = \mathbf{A}_i\mathbf{x} \ , \ i \in \{L,R\}, \tag{17}$$

where

$$\mathbf{x} := \begin{bmatrix} \mathbf{y}_i \\ \dot{\mathbf{y}}_i \end{bmatrix} \text{ and } \mathbf{A}_i = \begin{bmatrix} \mathbf{0}_{3\times3} & \mathbf{I}_{3\times3} \\ -\mathbf{K}_{Pi} & -\mathbf{K}_{Di} \end{bmatrix}. \tag{18}$$

Choose $\mathbf{K}_{Pi}$ and $\mathbf{K}_{Di}$ such that $\mathbf{A}_i$ is Hurwitz. Then for any real positive-definite-symmetric matrix $\mathbf{Q}_i$ ($i \in \{L,R\}$), there exists a real positive-definite-symmetric matrix $\mathbf{P}_i$, which is the unique solution to the Lyapunov equation defined by $\mathbf{A}_i$ and $\mathbf{Q}_i$. $V_i(\mathbf{x}) = \mathbf{x}^T\mathbf{P}_i\mathbf{x}$ is then a Lyapunov function candidate for the continuous-phase dynamics $\dot{\mathbf{x}} = \mathbf{A}_i\mathbf{x}$ [17], and there exist positive constants c_{1i}, c_{2i}, $c_{3i} > 0$ ($i \in \{L,R\}$) such that for all $\mathbf{x}$, $V_i(\mathbf{x})$ satisfies

$$c_{1i}||\mathbf{x}||^2 \le V_i(\mathbf{x}) \le c_{2i}||\mathbf{x}||^2, \dot{V}_i(\mathbf{x}) \le -c_{3i}V_i(\mathbf{x}). \tag{19}$$

Then, during each continuous phase, for all $\mathbf{x}$ with the initial state $\mathbf{x}_0$ at $t = t_0$,

$$V_i(\mathbf{x}) \le e^{-c_{3i}(t-t_0)}V_i(\mathbf{x}_0), \ \forall t > t_0. \tag{20}$$

IV. Stability Analysis

Given the previous formulation, walking dynamics can be compactly written as:

$$\begin{cases} \dot{\mathbf{x}} = \mathbf{A}_i \mathbf{x} \text{ (single-support-phase)} , \\ \mathbf{x}^+ = \Delta_i(t_{i_k}^-, \mathbf{x}^-) \text{ (double-support-phase)} , \end{cases} \tag{21}$$

where $i \in \{L,R\}$, $k \in \{1,2,...\}$, t_{L_k} and t_{R_k} represent the time instants when the k^{th} left-to-right-foot-support and the k^{th} right-to-left-foot-support impacts occur, respectively, and $\Delta_i(t_{i_k}^-, \mathbf{x}^-)$ can be derived from (5) and (10).

Theorem: There exist $\mathbf{K}_{Di}, \mathbf{K}_{Pi}, \delta > 0$ ($i \in \{L,R\}$) such that for any $\mathbf{x}(0) \in B_\delta(\mathbf{0}) = \{\mathbf{x} : ||\mathbf{x}|| < \delta\}$ the hybrid dynamical system (21) is exponentially stable.

Theorem proof is based on the construction of multiple Lyapunov functions [18]. Due to the space limitation, only the sketch of the proof is presented here.

Sketch of the proof: Let $V_L(\mathbf{x})$ and $V_R(\mathbf{x})$ be the Lyapunov functions associated with the left-foot-in-support and the right-foot-in-support phases, respectively. Suppose that walking begins with the left foot in support. Let $V_R|_K^+$ and $V_L|_{K+1}^+$ ($K \in \{1,3,5,...\}$) denote the values of Lyapunov functions right after the K^{th} and the $(K+1)^{th}$ impacts, respectively. By stability analysis via multiple Lyapunov functions, the overall system is exponentially stable, if $V_L(\mathbf{x})$ are $V_R(\mathbf{x})$ exponentially decreasing in the left-foot-in-support and the right-foot-in-support phases, respectively, and $\{V_R|_1^+, V_R|_3^+, V_R|_5^+ ...\}$ and $\{V_L|_2^+, V_L|_4^+, V_L|_6^+ ...\}$ are strictly decreasing sequences.

Because the continuous-phase subsystems are already exponentially stabilized under the controller design in Section III, we only need to derive stability conditions under which the sequences $\{V_R|_1^+, V_R|_3^+, V_R|_5^+ ...\}$ and $\{V_L|_2^+, V_L|_4^+, V_L|_6^+ ...\}$ are both strictly decreasing. This requirement can be rewritten as

$$V_R|_{K+2}^+ < V_R|_K^+ \text{ and } V_L|_{K+3}^+ < V_L|_{K+1}^+, \tag{22}$$

where

$$K \in \{1,3,5,...\}. \tag{23}$$

First, we prove that there exist $\mathbf{K}_{Pi}$ and $\mathbf{K}_{Di}$ ($i \in \{L,R\}$) such that $V_R|_{K+2}^+ < V_R|_K^+$.

Let ΔT_j denote the duration of the step right after the j^{th} impact ($j \in \{1,2,3,...\}$). From (20) we have

$$V_R|_{K+1}^- \le e^{-c_{3R}\Delta T_K} V_R|_K^+ \text{ and } V_L|_{K+2}^- \le e^{-c_{3L}\Delta T_{K+1}} V_L|_{K+1}^+. \tag{24}$$

Now consider the reset map $\Delta_i(t^-, \mathbf{x})$ ($i \in \{L,R\}$):

$$\begin{aligned} \|\mathbf{x}|_{K+1}^+\| &= \|\Delta_R(t_{K+1}^-, \mathbf{x}|_{K+1}^-)\| \\ &\le \|\Delta_R(t_{K+1}^-, \mathbf{x}|_{K+1}^-) - \Delta_R(t_{0_{K+1}}^-, \mathbf{x}|_{K+1}^-)\| \\ &+ \|\Delta_R(t_{0_{K+1}}^-, \mathbf{x}|_{K+1}^-) - \Delta_R(t_{0_{K+1}}^-, \mathbf{0})\|, \end{aligned} \tag{25}$$

where t_{K+1} is the time instant when the $(K+1)^{th}$ impact occurs, $\mathbf{x}|_{K+1}^-$ and $\mathbf{x}|_{K+1}^+$ denote the states right before and after the $(K+1)^{th}$ impact, respectively, and $t_{0_{K+1}}$ is the time instant when the $(K+1)^{th}$ impact occurs assuming that $\mathbf{x}(t) = 0$, $\forall t$. Note that $\Delta_L(t_{0_K}^-, \mathbf{0}) = \mathbf{0}$ and $\Delta_R(t_{0_{K+1}}^-, \mathbf{0}) = \mathbf{0}$ always hold if the desired gait is designed properly. It can be further proved that there exists $r^* > 0$ such that for any $\mathbf{x}|_{K+1}^- \in B_{r^*}(\mathbf{0})$ we have $\|\Delta_R(t_{0_{K+1}}^+, \mathbf{x}|_{K+1}^-) - \Delta_R(t_{0_{K+1}}^+, \mathbf{0})\| \le L_{\Delta_x}\|\mathbf{x}|_{K+1}^-\|$ and $\|\Delta_R(t_{K+1}^+, \mathbf{x}|_{K+1}^-) - \Delta_R(t_{0_{K+1}}^+, \mathbf{x}|_{K+1}^-)\| \le L_{\Delta_t}\|\mathbf{x}|_{K+1}^-\|$ where L_{Δ_x} and L_{Δ_t} are Lipschitz constants [19]. Due to the space limitation, detailed proof is not shown here. Therefore, we have

$$\|\mathbf{x}|_{K+1}^+\| \le L_{\Delta_R}\|\mathbf{x}|_{K+1}^-\|, \tag{26}$$

where $L_{\Delta_R} = L_{\Delta_t} + L_{\Delta_x}$.

Similarly,

$$\|\mathbf{x}|_{K+2}^+\| \le L_{\Delta_L}\|\mathbf{x}|_{K+2}^-\|, \tag{27}$$

where L_{Δ_L} is a Lipschitz constant.

According to (19), the following inequalities hold:

$$\begin{aligned} &V_R|_{K+1}^- \ge c_{1R}\|\mathbf{x}|_{K+1}^-\|^2, V_R|_{K+2}^+ \le c_{2R}\|\mathbf{x}|_{K+2}^+\|^2, \\ &V_L|_{K+1}^+ \le c_{2L}\|\mathbf{x}|_{K+1}^+\|^2, V_L|_{K+2}^- \ge c_{1L}\|\mathbf{x}|_{K+2}^-\|^2. \end{aligned} \tag{28}$$

Combining the above inequalities gives us

$$V_R|_{K+2}^+ \le \frac{c_{2L}c_{2R}}{c_{1R}c_{1L}} L_{\Delta_L}^2 L_{\Delta_R}^2 e^{-(c_{3L}\Delta T_{k+1} + c_{3R}\Delta T_K)} V_R|_K^+. \tag{29}$$

Let t_{sL} and t_{sR} denote the durations of a step during the left-leg-in-support and the right-leg-in-support phases assuming that $\mathbf{x} = 0$, $\forall t$, respectively. Due to the finite-time duration between two successive switching events, there exist positive numbers ε and l^* such that for all $\mathbf{x} \in B_{l^*}(\mathbf{0})$

$$|\Delta T_K - t_{sR}| \le \varepsilon t_{sR} \text{ and } |\Delta T_{K+1} - t_{sL}| \le \varepsilon t_{sL}. \tag{30}$$

Then we have,

$$V_R|_{K+2}^+ \le \frac{c_{2L}c_{2R}}{c_{1L}c_{1R}} L_{\Delta_L}^2 L_{\Delta_R}^2 e^{-(1-\varepsilon)(c_{3L}t_{sL} + c_{3R}t_{sR})} V_R|_K^+. \tag{31}$$

Similarly, it can be proved that

$$V_L|_{K+3}^+ \le \frac{c_{2L}c_{2R}}{c_{1L}c_{1R}} L_{\Delta_L}^2 L_{\Delta_R}^2 e^{-(1-\varepsilon)(c_{3L}t_{sL} + c_{3R}t_{sR})} V_L|_{K+1}^+. \tag{32}$$

Note that c_{3i} is determined by $\mathbf{K}_{Pi}$ and $\mathbf{K}_{Di}$. Hence, if there exist $\mathbf{K}_{Pi}$, $\mathbf{K}_{Di}$, $\delta > 0$ such that $\mathbf{A}_i$ is Hurwitz and that

$$c_{3L}t_{sL} + c_{3R}t_{sR} > \frac{1}{1-\varepsilon} \ln\left(\frac{c_{2L}c_{2R}}{c_{1L}c_{1R}} L_{\Delta_L}^2 L_{\Delta_R}^2\right) \tag{33}$$

holds for any $\mathbf{x}(0) \in B_\delta(\mathbf{0})$, then for any $K \in \{1,3,5,...\}$ we have $V_R|_{K+2}^+ < V_R|_K^+$ and $V_L|_{K+3}^+ < V_L|_{K+1}^+$ and the closed-loop system is exponentially stable. □

The stability condition in (33) indicates that the convergence rate should be sufficiently large such that divergence caused by the expansive impacts can be diminished.

An interesting question to ask here is, how different walking characterizations affect the stability condition in (33). Denote the reset map associated with the traditional gait characterization as $\tilde{\Delta}(t^-, \mathbf{x}^-)$. $\tilde{\Delta}(t^-, \mathbf{x}^-)$ is related to $\Delta_i(t^-, \mathbf{x}^-)$ through $\tilde{\Delta}(t^-, \mathbf{x}^-) = \mathbf{H}\Delta_i(t^-, \mathbf{x}^-)$, $i \in \{L,R\}$, where $\mathbf{H}$ is a projection matrix and represents the coordinate swap caused by role switching between the swing leg and the support leg. Because $\|\tilde{\Delta}(t, \mathbf{x})\| = \|\mathbf{H}\Delta_i(t, \mathbf{x})\| = \|\Delta_i(t, \mathbf{x})\|$ always holds, these two reset maps are equally expansive. Thus, changing the walking characterization does not affect the minimum rate of convergence for closed-loop stability.

V. Simulation Results

In this section, a 3-DOF biped walker with a compass gait is simulated to show the validity of the proposed stability condition based on the gait characterization and the walking

encoding method introduced in Section II. Two sets of simulation results are shown. The first one simulates asymmetric walking, and the second one shows a comparison between the proposed gait characterization and the traditional one.

A. Desired Gait Design

The desired gait defined by $s(t)-s_d(t)=0$ and $\mathbf{g}_i(\bar{s},\bar{\mathbf{q}})=\mathbf{0}$ is obtained through numerical search with the following constraints considered:

1) joint position and velocity limits;
2) joint-torque limits;
3) ground-contact constraints;
4) average walking speed;
5) the desired walking pattern of q_3 is $q_3=0$;
6) $\Delta_L(t_{0_K}^-,\mathbf{0})=\mathbf{0}$ and $\Delta_R(t_{0_{K+1}}^-,\mathbf{0})=\mathbf{0}$ with $K\in\{1,3,5,\ldots\}$.

The desired walking patterns generated through numerical search are shown in Fig. 3.

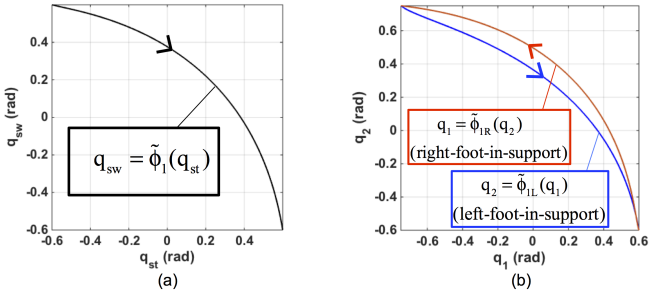

Fig. 3. Desired Walking Patterns. (a): symmetric. (b): asymmetric.

B. Stable Asymmetric Walking

Two sets of simulated asymmetric walking results with the walking pattern in Fig. 3(b) are presented with identical conditions except for the control parameters. Figure 4 shows the results with $\mathbf{K}_{Pi}=diag([21,28,28])$ and $\mathbf{K}_{Di}=diag([10,11,11])$, and Fig. 5 corresponds to $\mathbf{K}_{Pi}=diag([6,6,6])$ and $\mathbf{K}_{Di}=diag([5,5,5])$ $(i\in\{L,R\})$.

Exponentially stable walking is realized in both simulation results. From the time responses $q(t)$ (solid lines in Fig.4(a) and Fig.5(a)), it can be seen that the desired walking pattern is satisfactorily tracked. Plots (b) in both figures show that $s(t)$ tracks $s_d(t)$ exponentially fast. By comparing Fig. 4 with Fig. 5, we can see that the larger convergence rate during the continuous phases results in faster closed-loop convergence as predicted by the stability theorem in Section IV.

C. Stable Symmetric Walking: A Comparison with Traditional Walking Characterization

Symmetric walking with the walking pattern in Fig. 3(a) is simulated with the same initial conditions and control parameters but different walking characterizations. Figure 7 corresponds to the proposed characterization, where the left and the right legs are differentiated. Results with the traditional characterization are shown in Fig. 6. From Fig. 7(a), we can see that the joint positions become continuous upon impacts with the proposed characterization. On the contrary, the joint positions alway experience a jump when

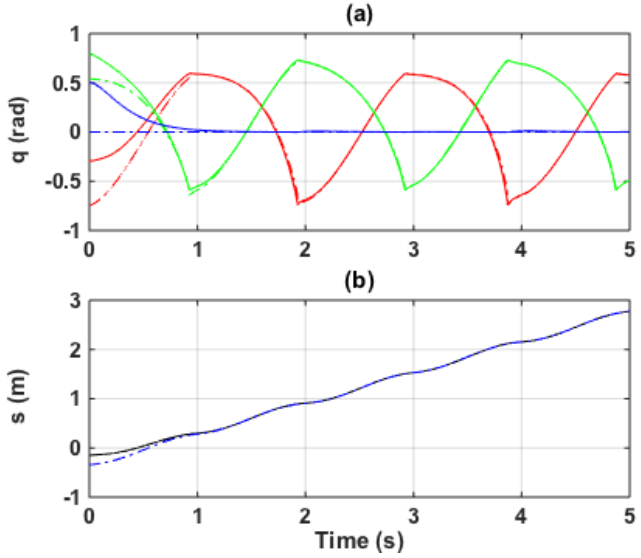

Fig. 4. Asymmetric Walking with $\mathbf{K}_{Pi}=diag([21,28,28])$ and $\mathbf{K}_{Di}=diag([10,11,11])$. Red line: left-leg angle q_1. Green line: right-leg angle q_2. Blue line: trunk angle q_3. Solid line: actual responses. Dashed line: desired trajectories determined by $\mathbf{g}_i(\bar{s},\bar{\mathbf{q}})=\mathbf{0}$ and $s_d(t)$.

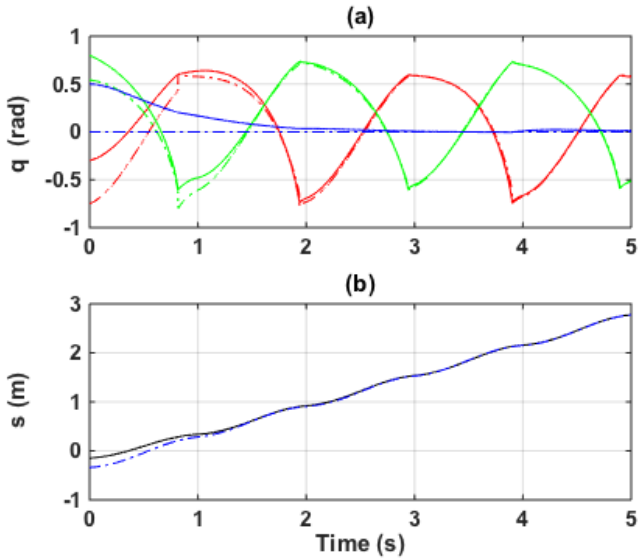

Fig. 5. Asymmetric Walking with $\mathbf{K}_{Pi}=diag([6,6,6])$ and $\mathbf{K}_{Di}=diag([5,5,5])$. Red line: left-leg angle q_1. Green line: right-leg angle q_2. Blue line: trunk angle q_3. Solid line: actual responses. Dashed line: desired trajectories determined by $\mathbf{g}_i(\bar{s},\bar{\mathbf{q}})=\mathbf{0}$ and $s_d(t)$.

the support leg and the swing leg switch their roles under the traditional walking characterization (see in Fig. 6(a)). As predicted in Section IV, the closed-loop convergence rates in these two simulations are the same because walking characterization does not affect the expansiveness of the reset map.

VI. Conclusions

In this paper, stable dynamic walking was studied based on recharacterization of bipedal gait and generalization of previous walking encoding. With the left leg differentiated from the right leg, an asymmetric walking pattern can be conveniently characterized. A biped's global position with

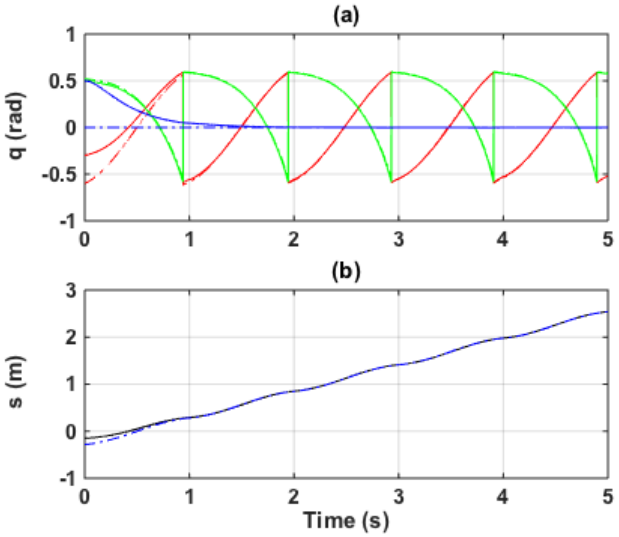

Fig. 6. Simulation Results with Walking Characterized by Support Leg and Swing Leg. Red line: support-leg angle q_{st}. Green line: swing-leg angle q_{sw}. Blue line: trunk angle q_3. Solid line: actual responses. Dashed line: desired trajectories determined by $\mathbf{g}_i(\bar{s},\bar{\mathbf{q}})=\mathbf{0}$ and $s_d(t)$.

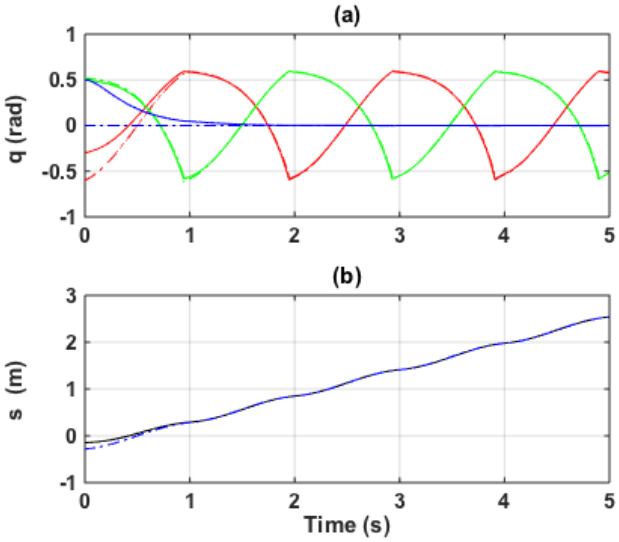

Fig. 7. Simulation Results with Walking Characterized by Left Leg and Right Leg. Red line: left-leg angle q_1. Green line: right-leg angle q_2. Blue line: trunk angle q_3. Solid line: actual responses. Dashed line: desired trajectories determined by $\mathbf{g}_i(\bar{s},\bar{\mathbf{q}})=\mathbf{0}$ and $s_d(t)$.

respect to the world coordinate frame is included in the set of generalized coordinates. The desired global motion can then be planned and tracked along with the desired walking pattern, which enables planning and control of high-level tasks such as multi-agent coordination. Controller design based on output feedback linearization is utilized to track the desired walking pattern and the desired global motion. Stability conditions of the closed-loop system are then analyzed via the construction of multiple Lyapunov functions. Planar compass-gait periodic walking is simulated for both an asymmetric gait and a symmetric gait. Simulation results showed that effective tracking of both the desired global motion and the desired walking pattern is achieved.

The results of this study can be extended to a bipedal gait with nonzero double-support phases and similar stability conditions still hold. The biped will be over-actuated during the double-support phases, which offers more control design freedoms. In our future research, the ground-contact constraints will be explicitly dealt with in the controller design, and other interesting problems such as underactuation and three-dimensional walking will be addressed.

REFERENCES

[1] P. Wieber, "On the stability of walking systems," in *Proc. Int. Workshop Humanoid Human Friendly Robot.*, 2002.

[2] J. P. Aubin, *Viability theory*. Springer, 2009.

[3] T. Koolen, T. De Boer, J. Rebula, A. Goswami, and J. Pratt, "Capturability-based analysis and control of legged locomotion, Part 1: Theory and application to three simple gait models," *Int. J. Robot. Research*, vol. 31, no. 9, pp. 1094–1113, 2012.

[4] J. E. Pratt, J. Carff, S. Drakunov, and A. Goswami, "Capture point: A step toward humanoid push recovery," in *Proc. IEEE Int. Conf. Humanoid Robot.*, 2006, pp. 200–207.

[5] J. Pratt, T. Koolen, T. De Boer, J. Rebula, S. Cotton, J. Carff, M. Johnson, and P. Neuhaus, "Capturability-based analysis and control of legged locomotion, part 2: Application to M2V2, a lower-body humanoid," *Int. J. Robot. Research*, vol. 31, no. 10, pp. 1117–1133, 2012.

[6] J. Grizzle, G. Abba, and P. Plestan, "Asymptotically stable walking for biped robots: Analysis via systems with impulse effects," *IEEE Trans. Autom. Control*, vol. 46, no. 1, pp. 51–64, 2001.

[7] B. Morris and J. W. Grizzle, "A restricted Poincaré map for determining exponentially stable periodic orbits in systems with impulse effects: Application to bipedal robots," in *Proc. IEEE Int. Conf. Decision Control*, 2005, pp. 4199–4206.

[8] A. D. Ames, K. Galloway, K. Sreenath, and J. W. Grizzle, "Rapidly exponentially stabilizing control Lyapunov functions and hybrid zero dynamics," *IEEE Trans. Autom. Control*, vol. 59, no. 4, pp. 876–891, 2014.

[9] A. Ramezani, J. W. Hurst, K. A. Hamed, and J. W. Grizzle, "Performance analysis and feedback control of atrias, a three-dimensional bipedal robot," *J. Dynamic Syst., Meas., Control*, vol. 136, no. 2, p. 021012, 2014.

[10] A. D. Ames, E. A. Cousineau, and M. J. Powell, "Dynamically stable bipedal robotic walking with nao via human-inspired hybrid zero dynamics," in *Proc. ACM Int. Conf. Hybrid Syst. Comput. Control*, 2012, pp. 135–144.

[11] B. G. Buss, A. Ramezani, K. A. Hamed, B. Griffin, K. S. Galloway, and J. W. e. a. Grizzle, "Preliminary walking experiments with underactuated 3d bipedal robot marlo," in *Proc. IEEE Int. Conf. Intell. Robot. Syst.*, 2014, pp. 2529–2536.

[12] I. R. Manchester, U. Mettin, F. Iida, and R. Tedrake, "Stable dynamic walking over uneven terrain," *Int. J. Robot. Research*, pp. 265–279, 2011.

[13] M. Posa, M. Tobenkin, and R. Tedrake, "Lyapunov analysis of rigid body systems with impacts and friction via sums-of-squares," in *Proc. of Int. Conf. Hybrid Syst. Comput. Control*, 2013, pp. 63–72.

[14] S. Rezazadeh and J. W. Hurst, "Toward step-by-step synthesis of stable gaits for underactuated compliant legged robots," in *Proc. IEEE Int. Conf. Robot. Automat.*, 2015, pp. 4532–4538.

[15] J. W. Grizzle, C. Chevallereau, R. W. Sinnet, and A. D. Ames, "Models, feedback control, and open problems of 3D bipedal robotic walking," *Automatica*, vol. 50, no. 8, pp. 1955–1988, 2014.

[16] B. Yao, C. Hu, and Q. Wang, "An orthogonal global task coordinate frame for contouring control of biaxial systems," *IEEE Trans. Mechatron.*, vol. 17, no. 4, pp. 622–634, 2012.

[17] H. K. Khalil, *Nonlinear control*. Prentice Hall, 1996.

[18] M. S. Branicky, "Multiple Lyapunov functions and other analysis tools for switched and hybrid systems," *IEEE Trans. Autom. Control*, vol. 43, no. 4, pp. 475–482, 1998.

[19] P. S. Simeonov and D. D. Bainov, "Exponential stability of the solutions of the initial-value problem for systems with impulse effect," *J. Comput. Appl. Math.*, vol. 23, no. 3, pp. 353–365, 1988.